IEEE Open Journal of Nanotechnology

Received 29 March 2024; revised 20 May 2024 and 14 June 2024; accepted 21 June 2024. Date of publication 25 June 2024; date of current version 12 July 2024. The review of this article was arranged by Associate Editor K. Nan.

Digital Object Identifier 10.1109/OJNANO.2024.3418840

Fully 3D Printed Miniaturized Electrochemical Platform With Plug-and-Play Graphitized Electrodes: Exhaustively Validated for Dopamine Sensing

K S JAYA LAKSHMI [1,3], RAMYA K [1,3], KHAIRUNNISA AMREEN [1,2], AND SANKET GOEL [1] (Senior Member, IEEE)

[1]Department of Electrical and Electronics Engineering, Birla Institute of Technology and Science (BITS) Pilani, Hyderabad 500078, India
[2]MEMS,Microfluidics and Nanoelectronics (MMNE) Lab, Birla Institute of Technology and Science(BITS) Pilani, Hyderabad 500078, India
[3]St. Anns College for Women-Mehdipatnam, Hyderabad 500028, India

CORRESPONDING AUTHOR: SANKET GOEL. (email: sgoel@hyderabad.bits-pilani.ac.in)

The work of Khairunnisa Amreen was supported by the DHR-ICMR Young Scientist Scheme under Grant YSS/2020/000086. This work was supported in part by DST-SERB Power Grant Program under Grant SPG/2021/001087 and in part by the Ministry of Science and Technology and Indo-Austria (WTZ), DST/IC/Austria/P-3/2021. *(K S Jaya Lakshmi and Ramya K contributed equally to this work.)*
This article has supplementary downloadable material available at https://doi.org/10.1109/OJNANO.2024.3418840, provided by the authors.

ABSTRACT Globally, a contemporary trend is towards the realization of sustainable, eco-friendly, miniaturized, and cost-effective sensors. This work focuses on developing a plug-and-play device using inexpensive and biodegradable UV resin fed 3D printing stereolithography (SLA) to produce miniaturized microfluidic platforms for electrochemical sensing. The device consists of three compartments designed to accommodate the 3-electrodes according to the need. SLA 3D printing technique solves these restrictions, making sensors reliable, repeatable, and durable. For electrochemical detection at the point of need or as a lab-on-chip (LoC) platform with minimal sample volume, this work attempts to construct a flexible as well as non-flexible microelectrode setup. The analytical capability of the platform is examined by quantifying nanomolar levels of dopamine in human body fluids. Chronoamperometry and cyclic voltammetry on surface-treated graphene-poly lactic acid (g-PLA) microelectrodes modified with gold nanoparticles are carried out utilizing a handheld potentiostat. The designed device has a linear range of 0.1 to 120 nM with limit of detection and limit of quantification of 0.083 and 0.27 nM, respectively. Various electrode characterizations, including scanning electron microscopy, energy-dispersive X-ray spectroscopy, and electrochemical impedance spectroscopy are carried out. The developed device is finally tested for real-time analysis on human blood and serum samples.

INDEX TERMS Stereolithography, 3D printing, plug-and-play microelectrodes, electrochemical sensing, microfluidics, point of need (pon), handheld portable potentiostat.

I. INTRODUCTION

The diminutive size of analytical apparatus is receiving a considerable attention in recent times. In comparison to conventional analytical systems, customized analytical equipment offers a multitude of benefits, such as diminished consumption of samples and reagents and refuse generation, thereby reducing the environmental impact of the analysis. Another feature is portability, and which allows to do analyses anywhere, including remote locations [1], [2]. Microfluidics is an interdisciplinary field that combines the disciplines of physics, chemistry, medicine, biology, and tissue engineering to manipulate small sample volumes quickly, enabling the investigation and replication of flow patterns in systems [3]. Microfluidics is crucial for preciseinvestigations of blood flow to replicate biological processes, necessitating the use of three dimensional (3D) geometries made from biocompatible materials [4], [5]. 3D printing, also known as additive manufacturing, is commonly used to create microfluidic

channels due to its benefits: (1) decreased time as well as cost for production, (2) ability to achieve micrometer-scale bare minimum feature size for appropriate dimensions, and (3) unrestricted creation of complex 3D shapes. Complicated 3D microfluidic channels with microelectrodes compartments can be produced using the 3D printing approach without the need for additional processes like casting as well as bonding on a large scale at a reproducible and inexpensive cost [6], [7]. Although layer-by-layer deposition process in 3D printing has its limitations, this technology provides distinct benefits such as expedited prototype, adaptable design, and customization options that may surpass the slower throughput for applications such as microfluidic sensing. As the advancement of 3D printing technology progresses, there will likely be attempts to increase printing speed without compromising on quality. This will contribute to narrowing the gap in throughput compared to traditional batch processes like soft lithography [8].

Common 3D printing methods include stereolithography (SLA) as well as fused deposition modeling (FDM). The product is created by selectively exposing a photocurable liquid resin to light in order to polymerize it. The layers may be carefully solidified and then put on top of each other using firm adherence till the product of choice is formed. SLA-based 3D printing offers high resolution ranging from 25 to 100 μm over FDM, ensuring accurate layer depositions and producing a refined finish on the printed structure [4], [9].Soft lithography involving Polydimethylsiloxane (PDMS) is also been widely employed in the fabrication of microfluidic devices owing to its inert properties, biocompatibility, and ability to transmit light [10]. The fabrication process with PDMS entails skillful execution and underscores the valuable expertise needed to ensure the best possible results [11]. The concluding stage in the assembly process of the microfluidic chip involves utilizing plasma-assisted bonding to join the cured PDMS material onto a glass slide [12], [13]. This is then followed by the incorporation of inlet and outlet ports, along with tubing connections. The intrinsic hydrophobicity of PDMS can be temporarily overcome by plasma exposure, but this solution won't be long-lasting. Additionally, it is the ability to absorb minuscule molecules, which might result in surface contamination. This is a significant issue in the field of biological investigations. When it comes to acids, bases, and solvents, PDMS isn't very compatible. The integrity of the microfluidic device and the experimental conditions could be compromised if these substances cause PDMS to swell or dissolve. Water evaporation through PDMS and a lower zeta potential than glass are two further drawbacks [14], [15], [16].

To overcome these limitations, UV resin 3D printing (SLA) is used for the fabrication of microfluidic devices. SLA can produce high-resolution microfluidic structures in both vertical and horizontal directions of the device. When it comes with sensing in microfluidic platforms, electrochemical analysis stands out. It is fully compatible with miniaturization, especially with the fabrication of microdevices and the use of handheld potentiostats. Additionally, it offers satisfactory selectivity and sensitivity through an appropriate selection of instrumental parameters as well as electrode material [17], [18], [19]. The primary electrodes utilized in electrochemical detection are noble metals, including gold and platinum, as well as carbon-based compounds [20]. Poly lactic acid (PLA) is a thermoplastic polymer that is biodegradable and biocompatible. PLA with carbon-based composites is used in several electrochemical sensors, the incorporation of graphene with PLA filament (g-PLA, a conductive filament) which is commercially available that are used for 3D printing (FDM) technique is shown to increase the conductivity of PLA and are selective towards the dopamine (DA) detection [21]. Commercially marketed conductive filaments have a low graphene weight percentage. One issue in employing 3D printed (FDM) g-PLA electrodes is to guarantee that enough electroactive material remains on their surface. Plasma treatment must be conducted on the 3D printed (FDM) g-PLA filament with low-pressure Oxygen. The oxygen plasma treatment has notably enhanced the conductivity of the g-PLA filament [22], [23].

Metallic nanoparticles (mNPs) have gained prominence as a highly promising material and have been extensively utilized in various domains, including sensing and catalysis, biolabeling as well as optoelectronics, owing to their distinctive properties [24]. Of all the mNPs, gold nanoparticles (AuNPs) have been extensively used in biosensors owing to their high conductivity and catalytic activity. The modification of g-PLA with electrodeposited AuNPs led to improved optical, electronic, and catalytic properties of the electrode. AuNP with Graphene or carbon fiber microelectrodes have been known to selectively determine DA in the presence of Ascorbic Acid (AA) [25]. The utilization of biodegradable photosensitive resins to produce an 3D printed (SLA) microfluidic device platform with three adjustable microelectrode compartments integrated with biocompatible and non-toxic g-PLA modified microelectrodes allows for the development of environmentally friendly and cost-effective sensors. Few of the examples where microfluidic devices is used for the electrochemical detection of DA based on low detection limit and wide linear range are consolidated and presented on Table S1 [26], [27], [28], [29], [30], [31].

The additional categories of electrode types that improve the performance of electrochemical sensing and can be easily connected and used in the developed platform are nanostructured electrodes, exemplified by carbon nanotubes and metal nanoparticles, offer unparalleled sensitivity, facilitating precise analytical detection. Composite electrodes, which seamlessly integrate conductive polymers with carbon materials, provide a harmonious balance of flexibility and stability, ensuring consistent performance across diverse environmental conditions. Screen-Printed Electrodes (SPEs) emerge as economical and adaptable solutions, particularly beneficial in diagnostic scenarios. Biofunctionalized electrodes, tailored with enzyme or aptamer modifications, guarantee specificity in biosensing applications. Surface-modified electrodes, utilizing self-assembled monolayers or plasma treatments, bolster both selectivity and reactivity, enhancing the accuracy of analyte detection. Additionally, the incorporation of

3D-printed and transparent electrodes, alongside magnetically modified variants, widens the scope of electrochemical applications, encompassing realms from medical diagnostics to environmental monitoring. These diverse electrode classes collectively contribute to advancing the capabilities and versatility of the developed sensing platform.

This work proposes a novel, straightforward, and cost-effective electrochemical microfluidic device capable of accommodating three micro electrodes (working electrode (WE), counter electrode (CE), and pseudo-reference electrode (RE)), fabricated on an 3D printed (SLA) substrate. The device, which is constructed from biodegradable material (photocurable liquid resin) featuring compact dimensions and adjustable microcompartments, offers a platform that aligns with the principles of Green and Sustainable Analytical Chemistry. This adaptive sensor exhibited exceptional performance and durability, presenting various possible applications. The device is demonstrated to detect dopamine in human body fluids using surface treated g-PLA modified microelectrodes as a proof of concept.

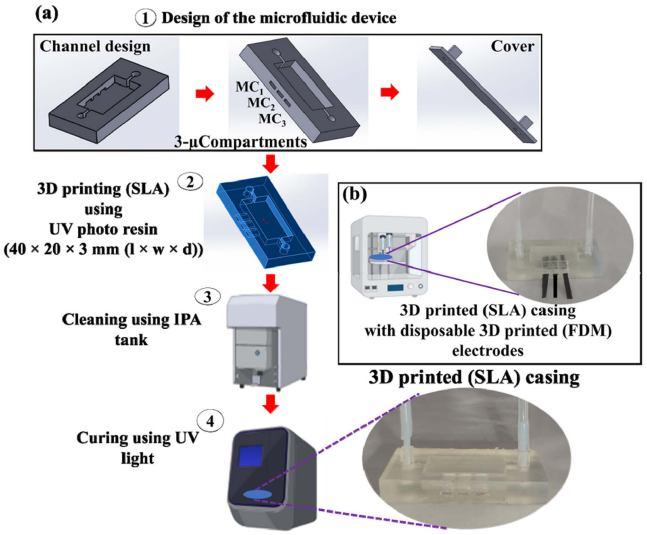

FIGURE 1. (a) Fabrication steps for 3D printed (SLA) microfluidic device casing with three adjustable microelectrode compartments and inlet/outlet ports; (b) 3D printed (SLA) casing with disposable 3D printed (FDM) electrodes.

II. EXPERIMENT

A. CHEMICALS AND APPARATUS

Dopamine Hydrochloride (DA > 98%), Uric Acid (UA, 99%), Ascorbic Acid (AA, 99%), Glucose (Glu, 99%), L-cysteine (L-Cys, 99%), Creatinine (Cre. 99%), Urea, Insulin from bovine pancreas, serotonin hydrochloride, Hypoxanthine (Hpx, 99%) and Tetra chloroauric (III) acid trihydrate 99% ($HAuCl_4.3H_2O$), melanin has been procured from Sigma Aldrich. Sodium Nitrite (NO_2^-99%) and Potassium Nitrate (NO_3^-99%) have been procured from SRL Chemicals, Conductive Graphene Composite PLA has been purchased from Black Magic 3D, USA. All the chemicals used are of scientific purity grade. All the electrochemical measurements are carried out using portable potentiostat (Sensit smart , PalmSens BV, The Netherlands), SPE connector (2 mm, PalmSens BV, The Netherlands) and bulk potentiostat (SP-150 BioLogic, France). Scanning Electron Microscopy (SEM) and Energy Dispersive X-Ray (EDX) techniques are carried out using Apreo scanning Electron microscope. Vacuum plasma system (CUTE, Femto Science, North Korea) is used for g-PLA surface treatment. For real sample analysis, human blood serum samples from single donor are obtained from Medical center of university campus.

B. FABRICATION AND ACTIVATION OF 3D PRINTED PLUG-AND-PLAY MICROFLUIDIC CASING WITH PLASMA G-PLA MICROELECTRODES

The microfluidic device is fabricated utilizing clear Resin (Form labs,V4, USA), a commercially available resin, employing a cost-effective approach based on 3D printing (SLA) technique. The printer is furnished with X-axis, Y-axis and Z-axis, which are responsible for controlling the positioning of objects on the developing platform as well as operate based on the coordinate system (cartesian). The resolution of the printer is limited by the size of the laser spot, whose measurement is of 140 μm in the XY-plane, and the thickness of each layer is 25 μm in the Z- direction. The microfluidic device (rectangular) is of 40 mm in length (l) and 20 mm in width (w) with a channel dimension of length (20 mm) and depth (3 mm, d). The device is initially created using a licensed computer-aided design (CAD) software (AutoCAD, Autodesk, Inc., California, USA) using the above-mentioned dimensions, to create a three-dimensional (3D) model. Furthermore, the device incorporates three adaptable microelectrode compartments (MC_1, MC_2 and MC_3) that facilitate the integration of the 3-electrode into the device. The resulting file is stored in the". stl" file format. The software-Form Labs, is employed to execute layer optimization, resulting in the successful execution of the printing procedure. The additional parts are removed after the printing process and cured. The developed device is cleaned for 15-minute using isopropyl alcohol (IPA) tank and cured at 60 °C for 5 minutes as depicted in the Fig. 1(a).

3D printed (FDM) technique (Fig. 1(b)) is used for the fabrication of g-PLA filament-based electrodes. The first step is to model the 3D desired design of g-PLA micro electrodes using the licensed computer software AutoCAD. The 3 microelectrodes WE, CE and RE are designed as rectangular sheets with dimensions of 20 mm × 3 mm and a thickness (t) of 1 mm as shown in Fig. 2. Then, the filaments are loaded in the printer and proper bed levelling are ensured before printing. The computer designed microelectrodes printing process is facilitated using FDM based 3D printer (Creator pro Flashforge, Zhejiang, China), employing an extrusion temperature of 220 °C and a nozzle speed of 45 mm/s. The bed temperature is set to 60 °C, while the nozzle diameter measured 0.4 mm via the open slicing software FlashPrint 5.0 (FlashForge corporation, China). The surface of printed g-PLA undergoes plasma

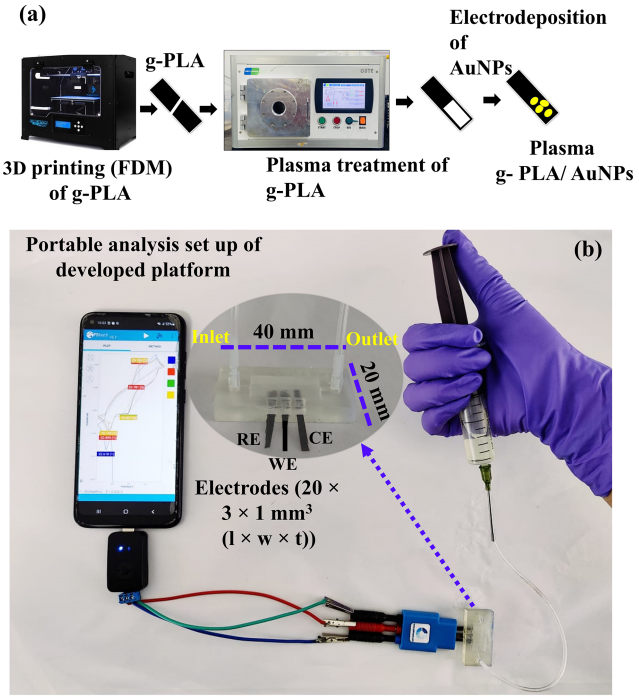

FIGURE 2. (a) Schematic for the surface treatment and synthesis of plasma g-PLA/ AuNPs and its electrochemical investigations; (b) Fully 3D-printed miniaturized electrochemical platform with plug-and-play electrodes.

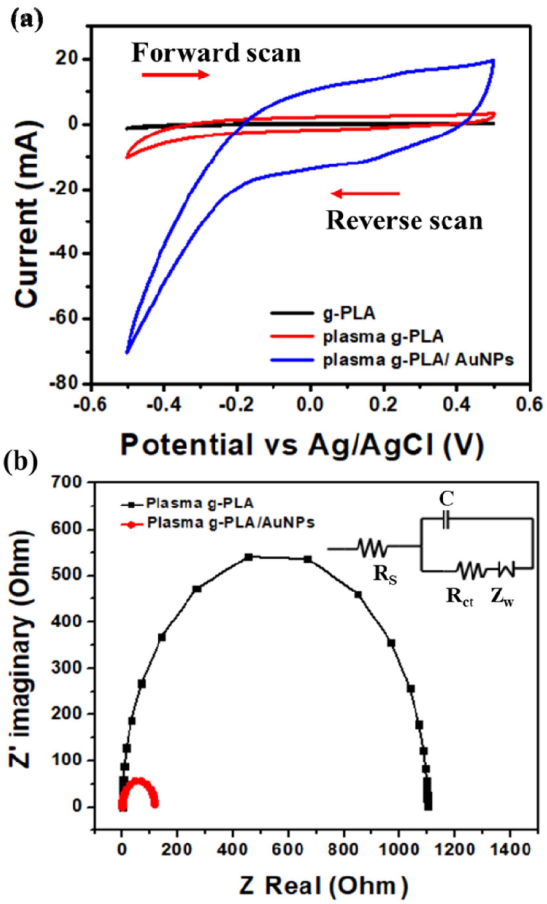

FIGURE 3. (a) CV response of g-PLA, plasma g-PLA device before and after electrodeposition of AuNPs; (b) Nyquist plots of plasma g-PLA and modified plasma g-PLA at 2V amplitude. Inset: corresponding randles sequence circuit.

treatment to activate it and enhance the materials adhesion capabilities, enabling improved bonding with the materials to be coated. This surface treatment is performed using Vacuum Plasma chamber (Femto Science, Gyeonggido, South Korea) by securely positioning the g-PLA on the sample carrier under a pressure of 1 bar and for a duration of 7 minutes to achieve adhesion as well as long term stability (Fig. 2).

C. SYNTHESIS AND OPTIMIZATION OF GOLD NANOPARTICLES (AUNPS)

The surface treated, plasma g-PLA is used for electrodeposition of AuNPs. The electrochemical technique involved the deposition of gold nanoparticles onto the working area of plasma g-PLA by reduction of 16.23 mM $HAuCl_4$. $3H_2O$.Multiple volumes (4, 8, 12, and 16 μL) of $HAuCl_4.3H_2O$ solution is deposited over the active region of a plasma-treated g-PLA substrate. This is conducted to establish the ideal volume necessary for effective electrodeposition (Fig. 2(a)). The electro deposition technique is carried out using cyclic voltammetry (CV) with a potential range of -1 to 1 V and a scan rate of 20 mVs^{-1}, using PBS (pH = 7) as an electrolyte for 40 cycles until the reduction peak of Au appeared. Fig. S1. (a) indicates that a volume of 12 μL of $HAuCl_4.3H_2O$ shows the best characteristics for effective electrodeposition, as seen by the increased background current. This g-PLA/AuNPs is further used as WE, g-PLA/Ag-AgCl is used as RE and g-PLA alone is used as CE for electrochemical analysis using a SPE connector [32], portable potentiostat [33] and smartphone as shown in (Fig. 2(b)).

III. RESULTS AND DISCUSSIONS

A. ELECTROCHEMICAL MEASUREMENTS

CV of the electrodeposition of AuNPs have been shown in Fig. S1 (b). The appearance of the oxidation as well as reduction peaks indicate the formation of AuNPs on plasma g-PLA.CV experiments are performed on the fabricated microfluidic device at a scan rate of 20 mVs^{-1} under a pH of 7 using PBS as the electrolyte solution. Fig. 3(a) depicts the CV of g-PLA, plasma g-PLA before and after the electrodeposition. It is evident that the baseline current of the plasma g-PLA/AuNPs in PBS solution is significantly higher compared to that of plasma g-PLA. This can be attributed to the distinctive catalytic and electrical characteristics of AuNPs present on the surface of plasma g-PLA, leading to an enhancement in area of the surface of the modified electrode thereby increasing the conductivity. Electrochemical Impedance spectroscopy (EIS) is an efficient electrochemical analysis tool for evaluating the physical characteristics of an active surface. It provides a reliable estimate of the

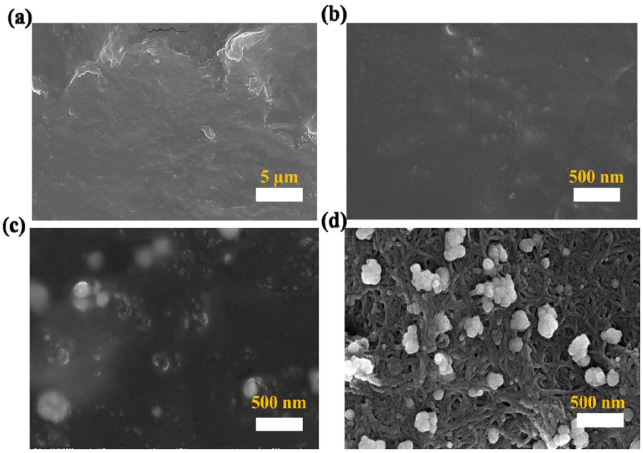

FIGURE 4. SEM morphology and EDAX spectra of (a, b) bare g-PLA, (c) plasma g-PLA, and (d) plasma g-PLA/ AuNPs.

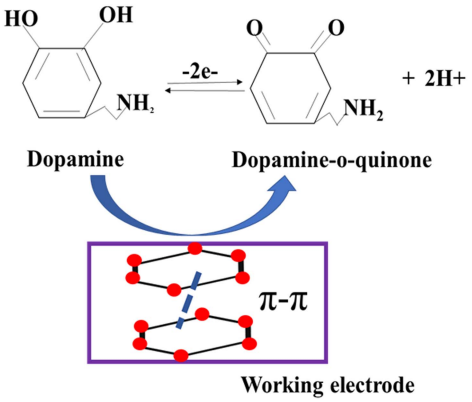

FIGURE 5. Electrochemical oxidation mechanism of dopamine on modified electrode.

charge transfer resistance (R_{ct}), which is mainly driven by the electron transfer process occurring between the electrolyte and the electrodes surface. The diameter of the semicircle obtained in the Nyquist plot is directly proportional to R_{ct} [34] . EIS is performed with a logarithmic frequency range of 1 Hz to 100 kHz and at an amplitude of 2V efficient and accurate characterization. The charge transfer resistance of the plasma PLA is decreased from 1110 Ω to 122 Ω indicating the high conductivity of the AuNPs and its Randles equivalent circuit fit is shown in the Fig. 3(b). Here, R_S refers to the electrolyte solution, R_{ct} represents the resistance to charge transfer resistance, and Z_W denotes the Warburg impedance. This impedance is caused by the movement of electroactive substances from the bulk solution to the surface of the electrode. The capacitance of the electrode surface/solution interface, denoted as C, represents the interfaces capacity to hold charge. It pertains to the formation of a double layer on the surface of the electrode caused by the adsorption of ions from the solution [35].

B. STRUCTURAL AND MORPHOLOGICAL ANALYSIS

Scanning Electron Microscopy (SEM) is used to analyze the morphological behavior in the surface of the electrodes. SEM image of untreated PLA in Fig. 4(a) and (b) displays a uniform composition with soft and smooth surface resulted because of its molecular structure and processing method used by manufacturer [36]. Following the plasma treatment, the surface material exhibits the presence of spots (Fig. 4(b)), which can be attributed to the elimination of impurities from the untreated g-PLA leading in the generation of surface roughness [37]. The spots on the plasma g-PLA have increased after the electrodeposition indicating the formation of AuNPs. The size of the deposited nanoparticles is found to be around 20–50 nm (Fig. 4(c)) which indicates effective deposition which results in increased catalytic activity. The observed phenomenon suggests that the electrodeposition is further enhanced the surface roughness of plasma g-PLA [38]. Energy-dispersive X-ray spectroscopy (EDAX) analysis of modified electrodes is listed in Table S2. Enrichment of oxygen is observed after plasma treatment indicating the efficacy of oxygen plasma treatment. The presence of Au spectra indicates the successful formation of AuNPs.

C. EFFECT OF SCAN RATE AND PH

When appropriate electrical voltage is applied to the plasma g-PLA/AuNPs, the compound DA undergoes oxidation to form DA-o-quinone as shown in Fig. 5. This process occurs through the shifting of two electrons as well as two protons. DA can engage in hydrogen bonding and electrostatic interactions with functional groups that are oxygenated on the electrode surface. Furthermore, the interaction between graphene aromatic rings and the DA can be facilitated by π–π stacking [38], [39]. These combined interactions result in a strong and stable binding of dopamine to the composite material. CV experiments are performed on the fabricated microfluidic device at a scan rate of 20 mVs^{-1} under a pH of 7 using PBS as the electrolyte solution. The measured amount of DA is altered during the experiment and the oxidation potential (E_{pa})is found to be 0.36 V as shown in Fig. 6(a). The impact of scan rate during the process of oxidation of DA with plasma g-PLA/AuNPs is investigated by varying scan rates ranging from 10 mVs^{-1} to 140 mVs^{-1} as depicted in Fig. S2. (a) in PBS (pH = 7) for 0.3 nM of DA. The experimental findings from Fig. 6(b) indicates a linear relationship between the anodic peak current as well as the scan rate, showing an increase in current. A linear correlation is determined between the different scan rates of the anodic current peak, referred to as I_{pa}, ($I_{pa} = 0.36x + 4.1$). Coefficient of correlation, R^2 is calculated to be 0.994. The results obtained demonstrate that the electrochemical analysis of the plasma g-PLA/ AuNPs integrated microfluidic device is facilitated by diffusion mechanism. The diffusion coefficient can be calculated by Randles Servick equation using the obtained slope 0.36.

$$I_{pa} = \left(2.69 \times 10^5\right).n^{3/2}.A.C.D^{1/2}.\upsilon^{1/2} \quad (1)$$

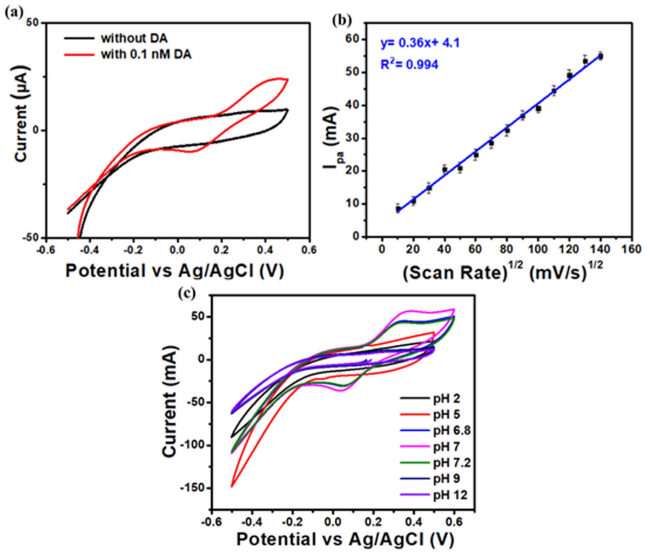

FIGURE 6. (a) CV response with and without DA in PBS (pH = 7) at 20 mVs^{-1}, (b) the peak current as function of square root of scan rate curves, and (c) CV of g-PLA/AuNPs in 0.3 nM of DA at 40 mVs^{-1} for varying pH (25, 6.87, 7.2, 912).

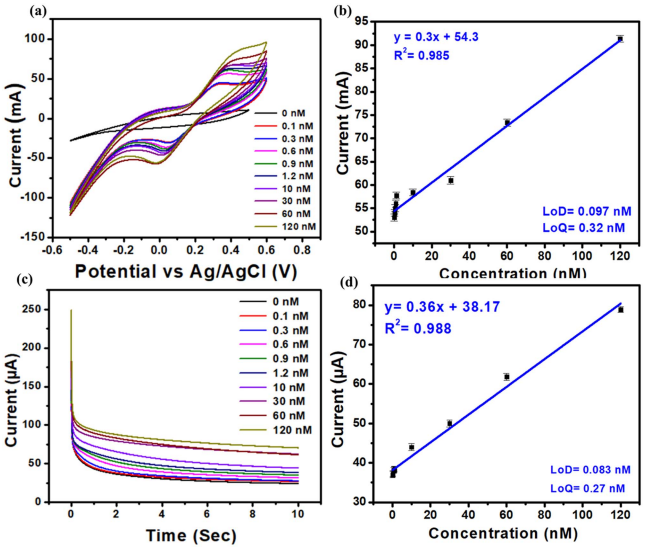

FIGURE 7. (a, b) CV for varying concentration of DA at 20 mVs^{-1} in PBS of pH = 7 and corresponding baseline corrected calibration plot, (c, d) CA response for increasing concentration of DA versus Ag/AgCl in pH = 7 PBS (at E_{pa} = 0.36 V) and corresponding baseline corrected calibration curve.

'I_{pa}' indicates Anodic peak current (the maximum current observed during the forward sweep of a cyclic voltammogram), 'n' indicates number of electrons transferred in the redox reaction., 'A' represents electrode surface area (in cm^2), 'C' indicates Concentration of the electroactive species (in mol/cm^3), 'D' is the diffusion coefficient of the electroactive species (in cm^2/s) and 'υ' is Scan rate (in V/s) [40].

A pH of 2–12 is used to evaluate the pH impact on the mechanism of the DA oxidation at the plasma g-PLA/AuNPs. The electrocatalytic behavior of DA is found to exhibit susceptibility to fluctuations in the pH levels of the electrolyte solution. From Fig. 6(c), it is evident that high peak current (at $E_{pa} = 0.36$ V) can be attributed to electrochemical anodic oxidation process taking place at a pH value of 7. At this specific pH level of 7, dopamine exhibits enhanced stability and mostly resides in its neutral state. This state of neutrality maximizes its capacity for oxidation, resulting in more distinct and well-defined electrochemical signals. Moreover, the relationship between dopamine along with the electrode surface is more favourable, resulting in improved adsorption as well as electron transfer rates. These combined factors contribute to the observed increase in sensitivity at neutral pH. Hence PBS at pH = 7 is considered suitable for DA detection ((Fig. S2 (b)).

D. ELECTROCHEMICAL DETECTION, INTERFERENCES STUDIES, REPEATABILITY AND REPRODUCIBILITY STUDIES

DA sensing is performed using the CV technique at a scan rate of 20 mV s^{-1} from −0.5 V to +0.5 V in PBS with a pH of 7. The concentration effect as well as the corresponding curve for calibration are illustrated in Fig. 7(a), (b). The current increased with rise in concentration, with a wide linear range of 0.1 nM to 120 nM, a quantification limit of 0.32 nM and a detection limit of 0.097 nM. The interference experiments are performed to validate the electrodes selectivity towards DA, which is a critical parameter for real-time detection in human body fluids. For this, Chronoamperometry (CA) is performed at 0.36 V (Fig. S3 (a)). Along with DA, many other electroactive substances found in the biological samples such as AA, Insulin, serotonin, NO_2^-, NO_3^-, L-Cys, Glu, Cre, Hpx,UA, melanin and cholesterol (Mix 1–11) are sequentially added ((Table S3). CA is carried out using 1 nM of DA and 5 folds of other analytes to maintain the ionic strength of the molecules. The currents obtained from the CA indicate that the sensor is selective towards DA with a standard deviation of 3.3.

The corresponding relative error bar diagram shown in Fig. 8(a) illustrates that the interferent species have a minimal impact on the current changes proving that plasma g-PLA/AuNPs can be used for the selective electrochemical determination of dopamine. Additionally, the concentration effect is assessed at 0.36 V using the CA technique. as illustrated in Fig. 7(c) and (d), a linear range of 0.1 nM to 120 nM is observed for DA ($R^2 = 0.987$).

The Limit of detection (LoD) as well as Limit of quantification (LoQ) is found to be 0.083 nM and 0.273 nM, respectively. Fig. S3. (b) shows the repeatability of 12 washes of plasma g-PLA/AuNPs. The study compared the CA signals from a 0.3 nM concentration of DA in PBS (pH = 7), it is therefore observed that the g-PLA/AuNPs in detecting dopamine remains relatively stable after multiple washes, but prolonged washing can compromise the robustness of g-PLA attachment to AuNPs due to physical agitation and buffer exposure. Variations in experimental conditions like temperature and agitation intensity during washing may further contribute to degradation of the g-PLA/AuNPs electrode modification and resulted in an acceptable RSD value of 1.7 (Fig. 8(b)). The reproducibility of the plasma g-PLA/AuNPs is assessed

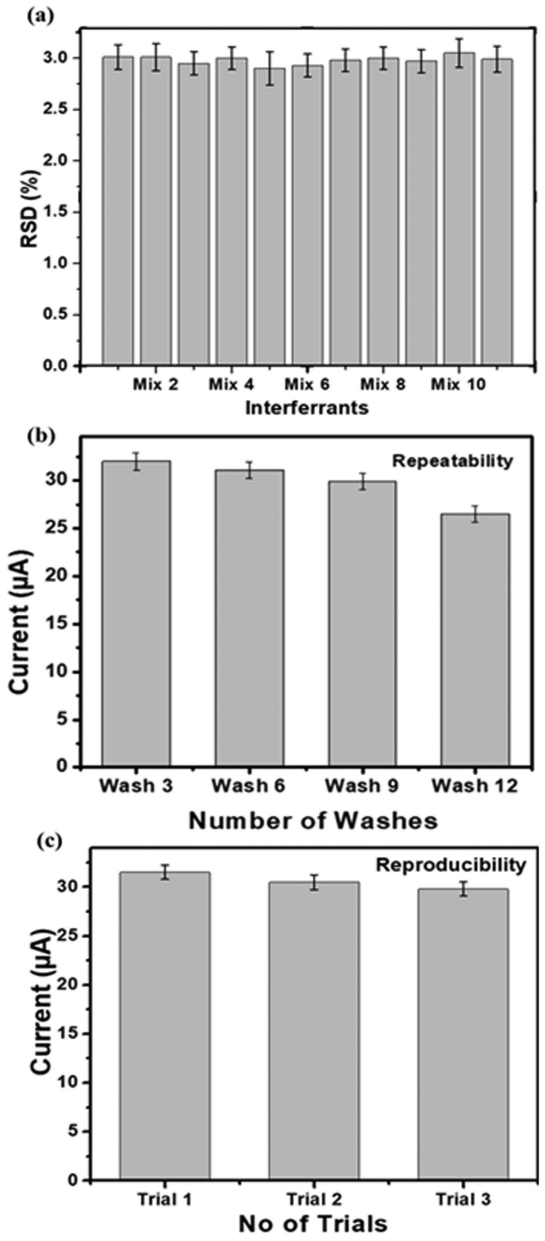

FIGURE 8. Error bar for (a) interference studies, (b) repeatability, and (c) reproducibility.

by conducting experiments with three sensors developed under similar conditions using CA technique as illustrated in Fig. S3. (c). The device showed a high level of reproducibility, as evidenced by error bar plot in Fig. 8(c). The observed variation of 1.6% between Trial 2 (device 2) and Trial 1 (device 1), and 3.8% between Trial 3 (device 3) and Trial 1 (device 1), falls within an acceptable range for research-grade analysis. These devices were fabricated under conditions aimed at ensuring consistency, yet slight differences in environmental factors like temperature and humidity may have influenced their performance. Such fluctuations can impact the behavior of electrochemical sensing devices, contributing to the slight observed variations in sensitivity among trials.

TABLE 1. Real Sample Validations of Plasma G-PLA/Aunps Microfluidic Device With Human Blood and Serum

Samples	Added (nM)	Found (nM)	Recovery (%)	RSD (%)
Blood	0	0.4	-	2.41
	10	10.5	105	2.53
	50	51	102	3.85
Serum	0	0.35	-	2.75
	10	9.8	98	3.12
	50	52	104	2.86

E. REAL SAMPLE VALIDATIONS

To analyse the applicability of the plasma g-PLA/ AuNPs microfluidic device, real sample analysis is performed using human blood and serum. The blood samples are collected from healthy volunteer. Serum samples are obtained by centrifuging the blood samples at 3500 RPM and stored at sub-zero temperatures until the moment of analysis. CA analysis is performed using the spiking technique. A fixed quantity of DA is added to individual portions, each containing 5 mL of a specific sample. The process of calculating DA recovery is executed utilizing the conventional method of addition. DA is introduced into each sample at different concentrations. The device demonstrated a high recovery rate ranging from 98% to 105%. The results, acquired through conducting three iterations, are presented in Table 1.

IV. CONCLUSION

A first attempt to introduce an innovative, simple, and affordable (2 USD per device platform) electrochemical microfluidic device that can hold three micro electrodes (working, counter, and pseudo-reference) fabricated using 3D printing (SLA) technique. The device is made from biodegradable material (photocurable liquid resin) with compact dimensions and adjustable microcompartments aligning with the principles of UN sustainable development goals (SDGs) and green chemistry (SDG 3-Good Health and Well-being and SDG 12-Sustainable Consumption and Production). This research work also offers the benefit of creating a design that can be interchanged with various types of electrodes, including flexible and non-flexible microelectrodes. This design allows for electrochemical detection as PoN/LoC platform. It is compatible with low sample volumes and can be customized to the users preferred shape and dimension. The sensors quantitative sustainability is evaluated from quantifying DA in human body fluids using modified surface-treated g-PLA electrodes fabricated by 3D printed (FDM) technique. The plasma g-PLA/AuNPs successfully detected DA with an oxidation potential of 0.36 V. The LoD as well as LoQ are found to be 0.083 nM and 0.27 nM respectively. The device is further characterized by repeatability, reproducibility, and stability. The modified electrode is characterized by SEM, EDAX and EIS. Real sample analysis is also been performed on the

device which establishes that the plasma g-PLA/ AuNPs integrated microfluidic device can be used for the selective determination of DAto assess its suitability in real-time scenarios specifically by conducting tests using human blood and serum samples for onsite analysis. This developed platform has the capability to detect multiple analytes simultaneously. This can be achieved through additional adjustments and modifications made to the platforms surface for future studies.

ACKNOWLEDGMENT

The authors are grateful to the Central Analytical Laboratory of the BITS Pilani Hyderabad campus for their contribution to the characterization and fabrication of the sensor. The authors thanks Abhishek Kumar, Research scholar, MMNE lab, BITS Pilani Hyderabad campus for supporting us with 3D printing.

REFERENCES

[1] E. F. M. Gabriel, B. G. Lucca, G. R. M. Duarte, and W. K. T. Coltro, "Recent advances in toner-based microfluidic devices for bioanalytical applications," *Anal. Methods*, vol. 10, no. 25, pp. 2952–2962, Jul. 2018, doi: 10.1039/C8AY01095A.

[2] J. Wen, J. Xu, W. Huang, C. Chen, L. Bai, and Y. Cheng, "Integrated sensing arrays based on organic electrochemical transistors," *IEEE Open J. Nanotechnol.*, vol. 3, pp. 101–115, 2022, doi: 10.1109/OJNANO.2022.3215135.

[3] K. S. Elvira, X. C. I. Solvas, R. C. R. Wootton, and A. J. Demello, "The past, present and potential for microfluidic reactor technology in chemical synthesis," *Nature Chem.*, vol. 5, no. 11, pp. 905–915, Oct. 2013, doi: 10.1038/nchem.1753.

[4] S. Knowlton, C. H. Yu, F. Ersoy, S. Emadi, A. Khademhosseini, and S. Tasoglu, "3D-printed microfluidic chips with patterned, cell-laden hydrogel constructs," *Biofabrication*, vol. 8, no. 2, 2016, Art. no. 025019, doi: 10.1088/1758-5090/8/2/025019.

[5] K. Ramya, K. Amreen, I. Pronin, A. Karmanov, N. Yakushova, and S. Goel, "Emerging trends in microfluidic-assisted nanomaterial synthesis for their high-resolution gas sensing applications," *Nano Futures*, vol. 7, no. 3, Aug. 2023, Art. no. 032004, doi: 10.1088/2399-1984/ACE9A3.

[6] D. S. Rocha et al., "Sandpaper-based electrochemical devices assembled on a reusable 3D-printed holder to detect date rape drug in beverages," *Talanta*, vol. 232, Sep. 2021, Art. no. 122408, doi: 10.1016/j.talanta.2021.122408.

[7] U. S. Jayapiriya and S. Goel, "Additively manufactured microfluidic enzymatic biofuel cell with comb-like bioelectrodes," *Microfluid Nanofluidics*, vol. 27, no. 6, p. 36, Jun. 2023, doi: 10.1007/S10404-023-02648-1.

[8] H. K. Balakrishnan et al., "3D printing: An alternative microfabrication approach with unprecedented opportunities in design," *Anal. Chem.*, vol. 93, no. 1, pp. 350–366, 2021, doi: 10.1021/acs.analchem.0c04672.

[9] A. Abdalla and B. A. Patel, "Annual review of analytical chemistry 3D printed electrochemical sensors," *Annu. Rev. Anal. Chem. (Palo Alto, Calif.)*, vol. 14, pp. 47–63, 2021, doi: 10.1146/annurev-anchem-091120.

[10] A. Khademhosseini et al., "A soft lithographic approach to fabricate patterned microfluidic channels," *Anal. Chem.*, vol. 76, pp. 3675–3681, 2004, doi: 10.1021/ac035415s.

[11] G. G. Morbioli, N. C. Speller, and A. M. Stockton, "A practical guide to rapid-prototyping of PDMS-based microfluidic devices: A tutorial," *Anal. Chim Acta*, vol. 1135, pp. 150–174, Oct. 2020, doi: 10.1016/J.ACA.2020.09.013.

[12] K. Giri and C. W. Tsao, "Recent advances in thermoplastic microfluidic bonding," *Micromachines*, vol. 13, no. 3, Mar. 2022, Art. no. 486, doi: 10.3390/MI13030486.

[13] S. Hashmi, G. F. Batalha, C. J. Van Tyne, and B. S. Yilbas, *Comprehensive Materials Processing*. Elsevier, 2014.

[14] R. Mukhopadhyay, "When PDMS isn't the best. What are its weaknesses, and which other polymers can researchers add to their toolboxes?," *Anal. Chem.*, vol. 79, no. 9, pp. 3248–3253, 2007, doi: 10.1021/ac071903e.

[15] J. C. Love, J. R. Anderson, and G. M. Whitesides, "Fabrication of three-dimensional microfluidic systems by soft lithography," *MRS Bull.*, vol. 26, no. 7, pp. 523–530, 2001, doi: 10.1557/mrs2001.124.

[16] K. Raj M and S. Chakraborty, "PDMS microfluidics: A mini review," *J. Appl. Polym. Sci.*, vol. 137, no. 27, 2020, Art. no. 48958, doi: 10.1002/app.48958.

[17] B. M. D. C. Costa, S. Griveau, F. d'Orlye, F. Bedioui, J. A. F. da Silva, and A. Varenne, "Microchip electrophoresis and electrochemical detection: A review on a growing synergistic implementation," *Electrochimica Acta*, vol. 391, 2021, Art. no. 138928, doi: 10.1016/j.electacta.2021.138928.

[18] T. Sierra, A. G. Crevillen, and A. Escarpa, "Electrochemical detection based on nanomaterials in CE and microfluidic systems," *Electrophoresis*, vol. 40, no. 1, pp. 113–123, 2019, doi: 10.1002/elps.201800281.

[19] S. Punj, D. Sidhu, D. Bhattacharya, M. Wang, and P. K. Wong, "An electrochemical biosensor platform for rapid immunoanalysis of physiological fluids," *IEEE Open J. Nanotechnol.*, vol. 1, pp. 31–37, 2020, doi: 10.1109/OJNANO.2020.2997296.

[20] G. S. Wilson, "Electrochemistry: Principles, methods, and applications," *Bioelectrochemistry Bioenergetics*, vol. 34, no. 2, p. 427, 1994, doi: 10.1016/0302-4598(94)80039-1.

[21] C. Kalinke et al., "Comparison of activation processes for 3D printed PLA-graphene electrodes: Electrochemical properties and application for sensing of dopamine," *Analyst*, vol. 145, no. 4, pp. 1207–1218, 2020, doi: 10.1039/c9an01926j.

[22] E. H. Baran and H. Yildirim Erbil, "Surface modification of 3D printed PLA objects by fused deposition modeling: A review," *Colloids Interfaces*, vol. 3, no. 2, pp. 1–25, 2019, doi: 10.3390/colloids3020043.

[23] J. F. S. Pereira et al., "Reactive oxygen plasma treatment of 3D-printed carbon electrodes towards high-performance electrochemical sensors," *Sensors Actuators B Chem.*, vol. 347, 2021, Art. no. 130651, doi: 10.1016/j.snb.2021.130651.

[24] Y. Si and H. J. Lee, "Carbon nanomaterials and metallic nanoparticles-incorporated electrochemical sensors for small metabolites: Detection methodologies and applications," *Curr. Opin. Electrochemistry*, vol. 22, pp. 234–243, 2020, doi: 10.1016/j.coelec.2020.08.007.

[25] A. I. Gopalan, K. P. Lee, K. M. Manesh, P. Santhosh, J. H. Kim, and J. S. Kang, "Electrochemical determination of dopamine and ascorbic acid at a novel gold nanoparticles distributed poly (4-aminothiophenol) modified electrode," *Talanta*, vol. 71, no. 4, pp.1774–1781, 2007, doi: 10.1016/j.talanta.2006.08.026.

[26] Z. Liu et al., "Electrochemical sensor integrated microfluidic device for sensitive and simultaneous quantification of dopamine and 5-hydroxytryptamine," *Sensors Actuators B Chem.*, vol. 273, pp. 873–883, Nov. 2018, doi: 10.1016/J.SNB.2018.06.123.

[27] E. Roznіecka, M. Jonsson-Niedziolka, A. Celebanska, J. Niedziolka-Jonsson, and M. Opallo, "Selective electrochemical detection of dopamine in a microfluidic channel on carbon nanoparticulate electrodes," *Analyst*, vol. 139, no. 11, pp. 2896–2903, May 2014, doi: 10.1039/C3AN02207B.

[28] M. Senel et al., "Microfluidic electrochemical sensor for cerebrospinal fluid and blood dopamine detection in a mouse model of Parkinson's disease," *Anal. Chem.*, vol. 92, no. 18, pp. 12347–12355, Sep. 2020, doi: 10.1021/ACS.ANALCHEM.0C02032/ASSET/IMAGES/LARGE/AC0C02032_0005.JPEG.

[29] A. A. Dawoud, T. Kawaguchi, Y. Markushin, M. D. Porter, and R. Jankowiak, "Separation of catecholamines and dopamine-derived DNA adduct using a microfluidic device with electrochemical detection," *Sensors Actuators B Chem.*, vol. 120, no. 1, pp. 42–50, Dec. 2006, doi: 10.1016/J.SNB.2006.01.041.

[30] M. D. Wagh, R. H, P. S. Kumar, K. Amreen, S. K. Sahoo, and S. Goel, "Integrated microfluidic device with MXene enhanced laser-induced graphene bioelectrode for sensitive and selective electroanalytical detection of dopamine," *IEEE Sensors J.*, vol. 22, no. 14, pp. 14620–14627, Jul. 2022, doi: 10.1109/JSEN.2022.3182293.

[31] S. Nuh, A. Numnuam, P. Thavarungkul, and T. Phairatana, "A novel microfluidic-based OMC-PEDOT-PSS composite electrochemical sensor for continuous dopamine monitoring," *Biosensors*, vol. 13, no. 1, Jan. 2023, Art. no. 68, doi: 10.3390/BIOS13010068/S1.

[32] [Online]. Available: https://www.palmsens.com/product/sensor-connector/

[33] [Online]. Available: https://www.palmsens.com/product/sensit-smart/

[34] D. Pan, Y. Gu, H. Lan, Y. Sun, and H. Gao, "Functional graphene-gold nano-composite fabricated electrochemical biosensor for direct and rapid detection of bisphenol A," *Anal. Chim. Acta*, vol. 853, no. 1, pp. 297–302, 2015, doi: 10.1016/j.aca.2014.11.004.

[35] G. Evtugyn et al., "Impedimetric aptasensor for ochratoxin a determination based on Au nanoparticles stabilized with hyper-branched polymer," *Sensors*, vol. 13, no. 12, pp. 16129–16145, 2013, doi: 10.3390/s131216129.

[36] M. Bhaiyya, P. Rewatkar, P. K. Pattnaik, and S. Goel, "Novel 3D printed single electrode-based portable and miniaturized electrochemiluminescence platform to detect lactate from human serum," *J. Micromechanics Microengineering*, vol. 33, no. 2, 2023, Art. no. 024001, doi: 10.1088/1361-6439/acac3e.

[37] A. Jordá-Vilaplana, V. Fombuena, D. García-García, M. D. Samper, and L. Sánchez-Nácher, "Surface modification of polylactic acid (PLA) by air atmospheric plasma treatment," *Eur. Polym. J.*, vol. 58, pp. 23–33, 2014, doi: 10.1016/j.eurpolymj.2014.06.002.

[38] P. Khashayar et al., "Characterization of gold nanoparticle layer deposited on gold electrode by various techniques for improved sensing abilities," *Biointerface Res. Appl. Chem.*, vol. 6, no. 4, pp. 1380–1390, 2016, Accessed: Feb. 22, 2024. [Online]. Available: http://hdl.handle.net/1854/LU-8086149

[39] E. Bahrami, R. Amini, and S. Vardak, "Electrochemical detection of dopamine via pencil graphite electrodes modified by Cu/CuxO nanoparticles," *J. Alloys Compd.*, vol. 855, 2021, Art. no. 157292, doi: 10.1016/j.jallcom.2020.157292.

[40] J. M. Mohan, S. Dudala, K. Amreen, A. Javed, S. K. Dubey, and S. Goel, "Microfluidic device integrated with PDMS microchannel and unmodified ITO glass electrodes for highly sensitive, specific, and point-of-care detection of copper and mercury," *IEEE Trans. Nanobiosci.*, vol. 22, no. 4, pp. 881–888, Oct. 2023, doi: 10.1109/TNB.2023.3241827.